An otolith-based back-calculation method to account for time-varying growth rate in rainbow smelt (*Osmerus mordax*) larvae[1]

Pascal Sirois, Frédéric Lecomte, and Julian J. Dodson

Abstract: This study develops a new back-calculation method, based on the larvae of rainbow smelt (*Osmerus mordax*), that takes into account the variation of growth rate over time. Known-aged larvae were reared in four 60-L microcosms during 49 days in order to obtain a large range of individual growth trajectories. We first validated the daily nature of the otolith increment deposition rate. The proposed time-varying growth (TVG) method weights the contribution of each increment in the length calculation using a growth effect factor. A small growth increment contributes less to the length increase of larvae than its relative importance in total otolith growth. On the other hand, a large growth increment contributes more to the length increase of larvae in comparison with its relative importance in total otolith growth. This method provided significantly better estimates of previous length-at-age than the biological intercept (BI) method at the individual level. In addition, the TVG method tended to provide more accurate estimates of previous length-at-age than the BI method at the population level, but the difference was not significant. The importance of using the TVG method instead of the BI method to back-calculate individual and population growth trajectories increases with the magnitude of the growth effect and the variation in growth rates over time.

Résumé : Cette étude présente une nouvelle méthode de rétrocalcul qui tient compte des variations temporelles du taux de croissance observées chez des larves d'éperlan arc-en-ciel (*Osmerus mordax*). Des larves d'un âge connu ont été élevées dans quatre microcosmes de 60 L pendant 49 jours dans le but d'obtenir un large éventail de trajectoires de croissance. Nous avons préalablement validé le dépôt journalier des accroissements sur les otolithes. La méthode des variations temporelles du taux de croissance (TVG) que nous proposons, corrige la contribution de chaque accroissement dans le calcul de la longueur en utilisant un facteur d'effet de croissance. Un petit accroissement contribue moins à l'augmentation de la longueur de la larve que son importance relative dans la taille de l'otolithe. De façon opposée, un grand accroissement contribue plus à l'augmentation de la longueur de la larve que son importance relative dans la taille de l'otolithe. Au niveau individuel, la méthode TVG a fourni de meilleures estimations de longueurs à des âges ultérieurs que la méthode de l'ordonnée à l'origine biologique (BI). De plus, au niveau des populations, la méthode TVG avait tendance à fournir de meilleures estimations de longueurs à des âges ultérieurs que la méthode BI, cependant la différence n'est pas significative. L'importance d'utiliser la méthode TVG au lieu de la méthode BI pour rétrocalculer les trajectoires de croissance des individus et des populations, croît avec l'augmentation de l'effet de croissance et des variations temporelles du taux de croissance.

Introduction

Back-calculation of fish lengths from bony structures has provided major contributions to fishery ecology by permitting the collection of individual longitudinal data series. Such series have been widely used to determine factors controlling recruitment. These studies focus on young individuals because small changes in their survival can lead to great variations in recruitment (Houde 1987).

Received May 22, 1998. Accepted October 16, 1998.
J14599

P. Sirois, F. Lecomte, and J.J. Dodson.[2] GIROQ, Département de Biologie, Université Laval, Québec, QC G1K 7P4, Canada.

[1]Contribution to the program of GIROQ (Groupe Interuniversitaire de Recherches Océanographiques du Québec).

[2]Author to whom all correspondence should be addressed. e-mail: julian.dodson@bio.ulaval.ca

Since the first utilization of back-calculation (Lea 1910), numerous methods have been developed to enhance length estimates (see review by Francis 1990). Most of these methods are based on two assumptions: (*i*) constant periodicity in the formation of the bony structure and (*ii*) proportionality between the growth of calcified structures and somatic growth. The first assumption has been demonstrated on daily and annual bases for a wide variety of fish species (Campana and Neilson 1985; Casselman 1987; Geffen 1992). It is nevertheless recommended that the deposition rate for each studied species be validated. The second assumption has never been demonstrated directly, but rather empirically using strong correlations between the size of the bony part and the size of the fish.

Many investigators have reported that the relationship between fish size and otolith size is at times weak or "uncoupled" (Marshall and Parker 1982; Volk et al. 1984; Rice et al. 1985; Mosegaard et al. 1988; Molony and Choat 1990; Wright et al. 1990; Bradford and Geen 1992; Secor and Dean 1992). The relationship between somatic growth and otolith growth has been demonstrated to be related to abso-

Fig. 1. Relationships between number of increments and age of individual rainbow smelt larvae sampled in four different microcosms (M1, M2, M3, and M4). Regression equations, R^2 values, and sample size (N) are reported on each graph. All panels are scaled similarly.

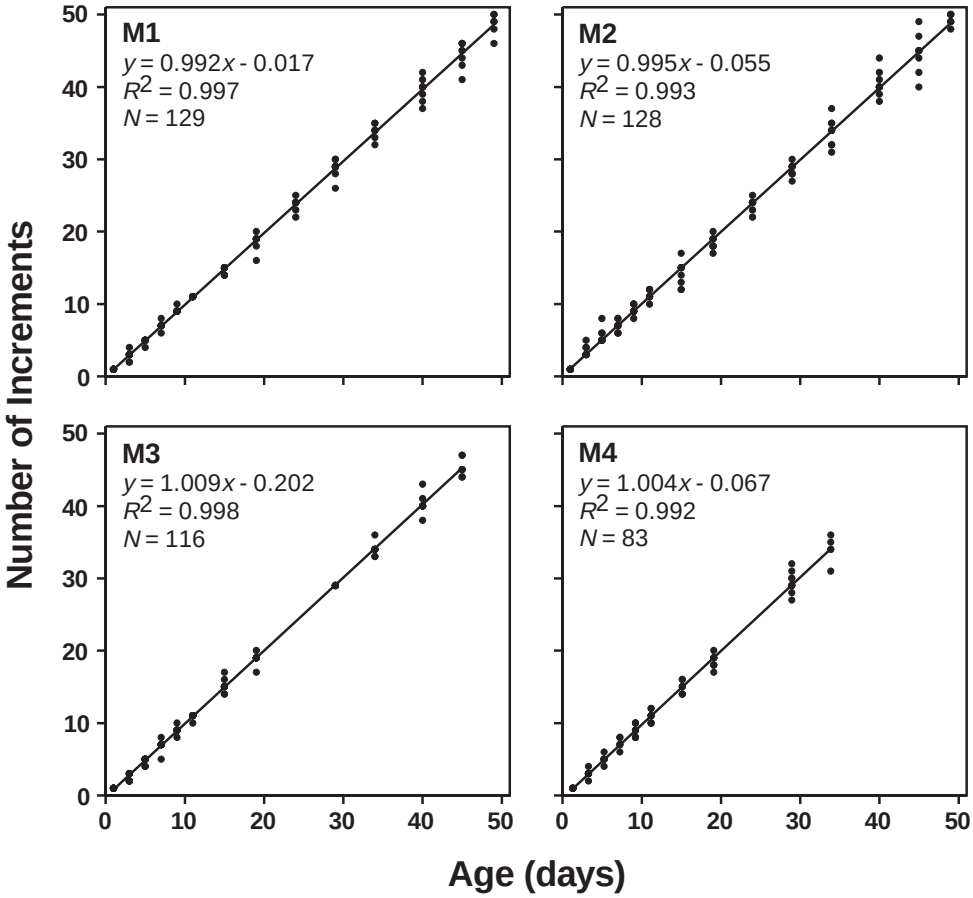

lute growth rate (Reznick et al. 1989; Secor and Dean 1989, 1992; Secor et al. 1989; Francis et al. 1993; Xiao 1996; Schirripa and Goodyear 1997). According to these studies, otoliths from slow-growing fish are larger than those from fast-growing fish of the same size. This phenomenon has been called the growth effect and may cause bias in length estimates when using traditional back-calculation methods (Campana 1990; Campana and Jones 1992). Campana (1990) proposed a biological intercept (BI) method to eliminate back-calculation bias caused by the growth effect. However, it has been shown that this method is sensitive to variations in growth rate over time (Campana 1990; Secor and Dean 1992). Growth rate variations are likely to appear during larval and juvenile stages owing to environmental variation or transition between early developmental stages.

The principal objective of this study was to develop a new back-calculation method, based on the larvae of rainbow smelt (*Osmerus mordax*), that takes into account the variation of growth rate over time. This method is based on the assumptions that (*i*) there is a daily periodicity in the formation of the otolith and (*ii*) there is a proportionality between somatic and otolith growth. However, the method assumes that the proportionality varies with somatic growth rate. Thus, the first step was to validate the otolith increment deposition rate for rainbow smelt larvae. We then developed an equation that weighted the contribution of each increment in the length calculation using a growth effect factor. Finally, we compared back-calculated lengths estimated using the proposed time-varying growth (TVG) method with those obtained with the BI method at the population level and at the individual level.

Table 1. Number of larvae sampled in microcosms on various dates.

Date	Days after hatch	No. of larvae sampled			
		M1	M2	M3	M4
May 24	1	10	10	10	10
May 26	3	10	10	10	10
May 28	5	10	10	10	10
May 30	7	10	10	10	10
June 1	9	10	10	10	10
June 3	11	10	10	10	10
June 7	15	10	10	10	10
June 11	19	10	10	10	10
June 16	24	10	10		
June 21	29	10	10	10	10
June 26	34	10	10	10	6
July 2	40	10	10	10	
July 7	45	10	10	7	
July 11	49	8	6		

Fig. 2. Observed standard length of individual rainbow smelt sampled at various ages in M1, M2, M3, and M4 with respective polynomial lines (solid lines) fit to the natural log-transformed data. M1: $\ln(y) = 1.85 + 0.0729x - 0.00764x^2 + 0.000358x^3 - 0.00000723x^4 + 0.0000000533x^5$; M2: $\ln(y) = 1.80 + 0.101x - 0.0120x^2 + 0.000625x^3 - 0.0000137x^4 + 0.000000108x^5$; M3: $\ln(y) = 1.77 + 0.116x - 0.0133x^2 + 0.000673x^3 - 0.0000144x^4 + 0.000000110x^5$; M4: $\ln(y) = 1.85 + 0.0792x - 0.00919x^2 + 0.000436x^3 - 0.00000604x^4$. The 95% confidence curves for individual estimates (dotted lines) are shown for each microcosm. R^2 values and sample size (N) are reported on each graph. All panels are scaled similarly.

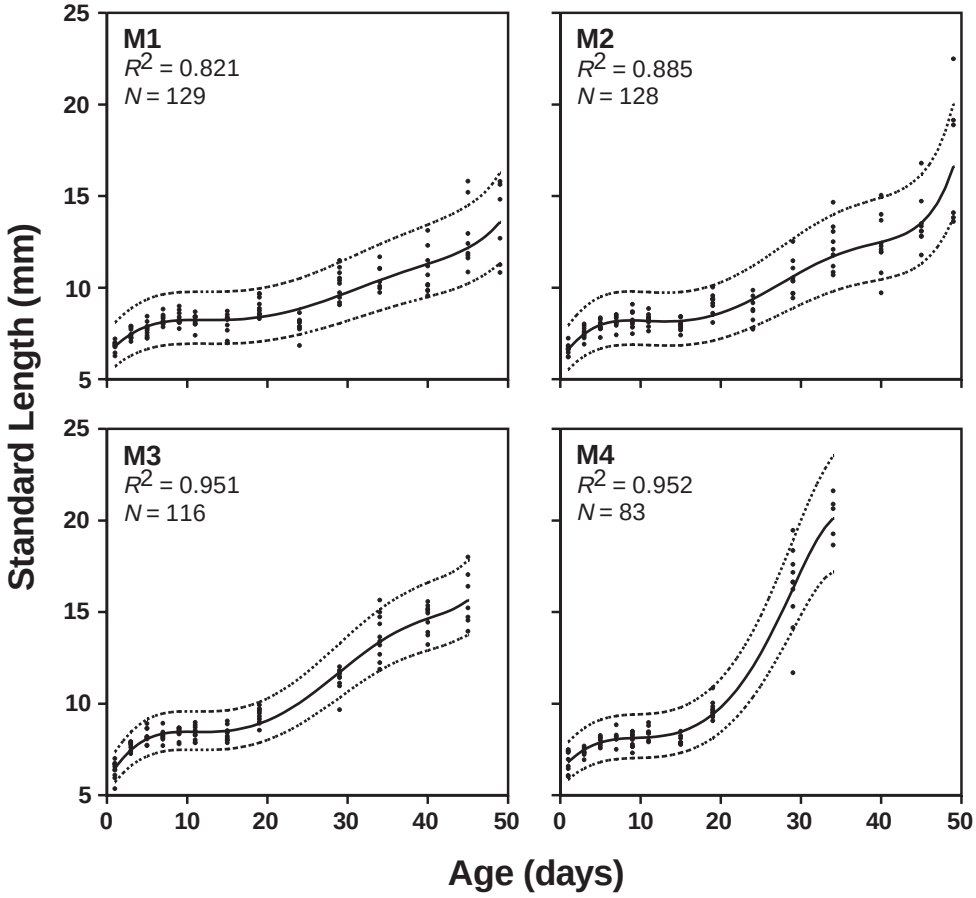

Materials and methods

Experimental procedure

A microcosm experiment was performed in order to obtain a large range of individual growth trajectories. Fertilized eggs of rainbow smelt were provided by an experimental incubator operated by the Ministère de l'Environnement et de la Faune (MEF, Quebec) on a well-known spawning site of this species (Ruisseau de l'Église, Beaumont, Quebec). On May 23, 1994, at night, large numbers of larvae hatched and were placed randomly in four 60-L microcosms (M1, M2, M3, and M4; height 55 cm, diameter 40 cm). Initial density of larvae varied from 16 to 22 ind.·L^{-1}. Known-age larvae were reared for 49 days. Microcosms were supplied with water pumped directly from the south shore of the St. Lawrence middle estuary. This region constitutes a major nursery area for rainbow smelt (Dodson et al. 1989; Laprise and Dodson 1989*a*, 1989*b*). Environmental conditions were similar among microcosms, but varied in time according to the natural changes of the variables in the wild. Temperature warmed gradually from 10.2 to 22.0°C, salinity fluctuated between 0 and 2.1 psu (practical salinity units), and turbidity ranged between 55 and 78 NTU (nephelometric turbidity units) during the experiment.

Natural food was present in the inflow water but was not sufficient to support the densities of larvae in the microcosms. Rations of wild-caught zooplankton were added to the tanks in order to account for higher larval densities. A ration (about 900 prey items) was added once per day in M1, twice per day in M2, three times per day in M3, and four times per day in M4.

Larvae were sampled at 2- to 6-day intervals (Table 1) and were preserved in 95% ethanol. Standard lengths were measured using an image analysis system. Shrinkage due to preservation in 95% ethanol was calculated on 30 rainbow smelt larvae ranging in length from 6.14 to 15.86 mm. Shrinkage varied from –7.04 to 5.33% and the mean was –1.12%. The 95% confidence interval around this mean ranged from –2.29 to 0.04% and thus was not significantly different from 0. For this reason, no correction for shrinkage due to preservation in ethanol was made.

Otolith microstructure procedure

Sagittal otoliths were removed with fine needles and mounted on a microscope slide with thermoplastic glue (Crystal Bond). Rainbow smelt larvae sagittae are small (mean otolith radius at hatching = 10.38 μm) and show clear and distinct growth increments. Otoliths were measured using an image analysis system connected to a light microscope at 630–1000× magnification. Three measurements were taken along the growth axis: core radius (micrometres), otolith radius (micrometres), and individual increment width (micrometres). The number of increments was automatically compiled using the number of widths measured. All otoliths were read in random order by two different readers. A total

Fig. 3. Observed otolith radius of individual rainbow smelt sampled at various ages in M1, M2, M3, and M4 with respective polynomial lines fit to the natural log-transformed data. M1: $\ln(y) = 2.41 + 0.0623x - 0.00154x^2 + 0.0000211x^3$; M2: $\ln(y) = 2.39 + 0.0623x - 0.00141x^2 + 0.0000224x^3$; M3: $\ln(y) = 2.34 + 0.113x - 0.00766x^2 + 0.000275x^3 - 0.00000303x^4$; M4: $\ln(y) = 2.32 + 0.126x - 0.0112x^2 + 0.000493x^3 - 0.00000619x^4$. R^2 values and sample size (N) are reported on each graph. All panels are scaled similarly.

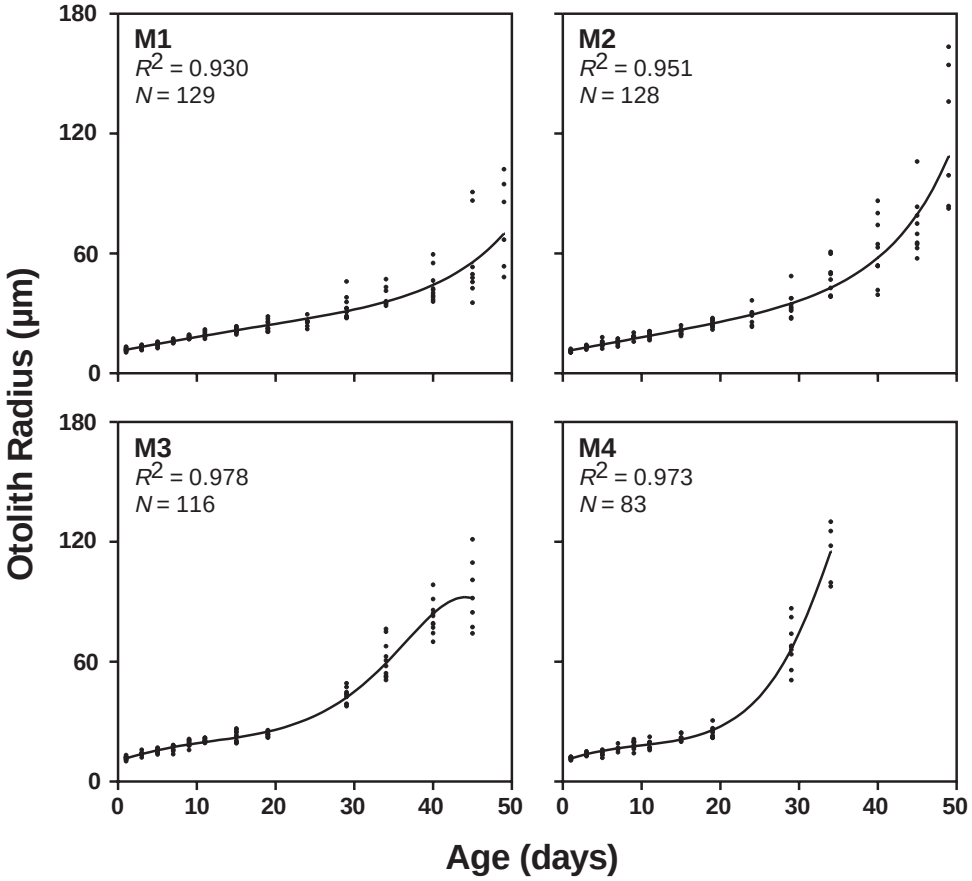

of 487 otoliths were examined and 31 (6.3%) were discarded from the analysis because of a discrepancy exceeding 10% in the number of increments between readers.

Computations

Computations involving standard length and otolith radius were executed on natural log-transformed data. The growth effect (R) was calculated by a linear regression using each individual fish as an independent observation (N = 456):

$$S = b + RG \quad (1)$$

where S is the estimated slope of the fish size – otolith size relationship, G is the absolute linear growth rate in fish length, and b and R (growth effect) are estimated parameters of the linear regression. For each fish, S was computed using standard length and otolith radius observed at capture, and standard length and otolith radius at hatching, which is the BI (see below). Similarly, G was calculated as the difference between the observed standard length at capture and the standard length at hatching divided by the number of daily growth increments obtained from otoliths.

All fish (N = 456) were used in the back-calculation analysis. For each fish, the body growth trajectory was back-calculated on every day lived in the microcosms using two different methods. First, the BI method provided length estimates using the following equation (Campana 1990):

$$L_t = L_c + (O_t - O_c)(L_c - L_0)(O_c - O_0)^{-1} \quad (2)$$

where L is fish length at age t (L_t), at the BI (L_0), and at capture (L_c) and O is otolith radius at age t (O_t), at the BI (O_0), and at capture (O_c). To determine L_0, measurements of rainbow smelt larvae within hours after hatching were recorded from an independent sample in the laboratory in 1995 and 1996. The mean standard length calculated on newly hatched rainbow smelt was 5.81 mm (SD = 0.41, N = 315). The O_0 was estimated using the observed core radius on the otolith of each larva.

The second method was developed using the structure of the BI method and a TVG simulation presented by Campana (1990). This method involves calculating a growth effect factor to correct the contribution of each increment to the body growth trajectory. Back-calculated lengths according to the TVG method were provided by

$$L_t = L_0 + \sum_{i=1}^{t} (W_t + R(W_t - W))(L_c - L_0)(O_c - O_0)^{-1} \quad (3)$$

where W_t is the increment width at age t and W is the mean increment width. Values of W were calculated for each fish during the yolk-sac stage (0–7 days), preflexion stage (8–30 days), and postflexion stage (31+ days). Developmental stages were determined in this study by laboratory observations and by the description of larval rainbow smelt development of Cooper (1978). Since rainbow smelt larvae reach the juvenile stage at about 36 mm, no larva became juvenile in this study.

Fig. 4. Relationships between standard length and otolith radius of individual rainbow smelt sampled at various ages in M1, M2, M3, and M4. Regression equations, R^2 values, and sample size (N) are reported on each graph. All panels are scaled similarly.

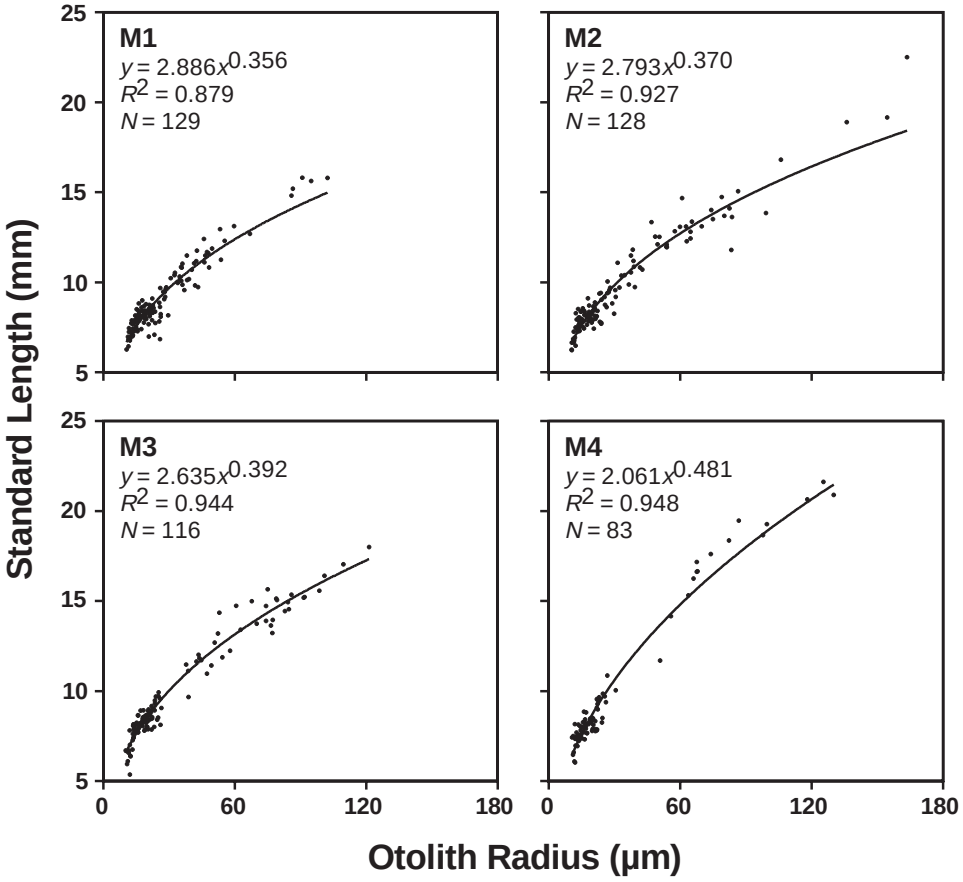

Statistical analysis

Regression slopes (number of increments versus age; mean back-calculated length versus mean observed length) were compared with the theoretical slope of 1 with a *t*-test using $\alpha = 0.05$ as the level of significance. The 95% confidence curves for individual estimates of the polynomial regression were calculated according to Neter et al. (1985). Slopes and elevations of the fish size – otolith size relationships were compared using an analysis of covariance (ANCOVA) and a Tukey multiple comparisons test (Zar 1987). Frequencies of back-calculated lengths observed within the 95% confidence curves of the fitted growth model were compared using a contingency table (Zar 1987).

Results

Validation of daily otolith increment deposition rate

Relationships between the number of increments and true age of the rainbow smelt larvae are shown for each microcosm in Fig. 1. Deposition rates, i.e., slopes of regressions, varied from 0.992 to 1.009 increments per day and were not significantly different from 1 in M1, M2, and M4. The slope of the regression is statistically different from 1 in M3 ($t_{114} = 1.995$, $p = 0.048$). However, this corresponds to one additional growth increment produced every 110 days, which is trivial. Intercepts were not significantly different from 0 in all microcosms ($p > 0.05$ in all cases). This result suggested that daily increment formation began at hatching,

Fig. 5. Relationship between the slope of the body size – otolith size relationship and the absolute body growth rate calculated using individual larvae sampled at various dates in M1, M2, M3, and M4. All larvae from all microcosms are pooled on the same graph.

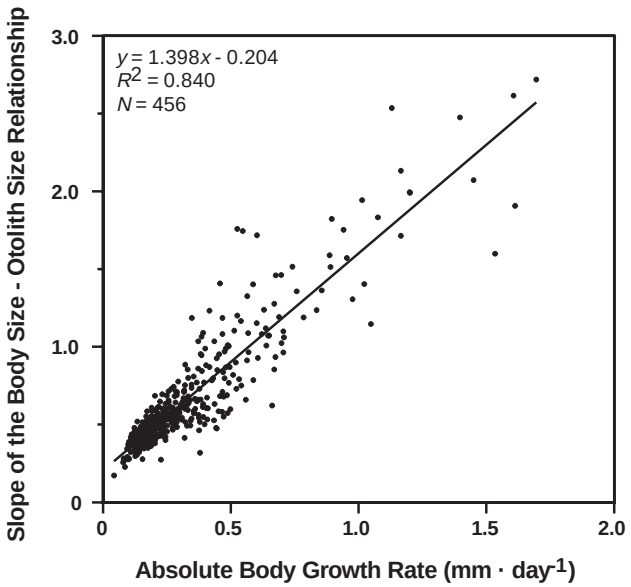

Fig. 6. Mean somatic growth trajectories as showed by the observed length (circles), the back-calculated length using the BI method (dotted lines), and the back-calculated length using the TVG method (solid lines) in M1, M2, M3, and M4. Vertical bars on observed lengths represent the SDs.

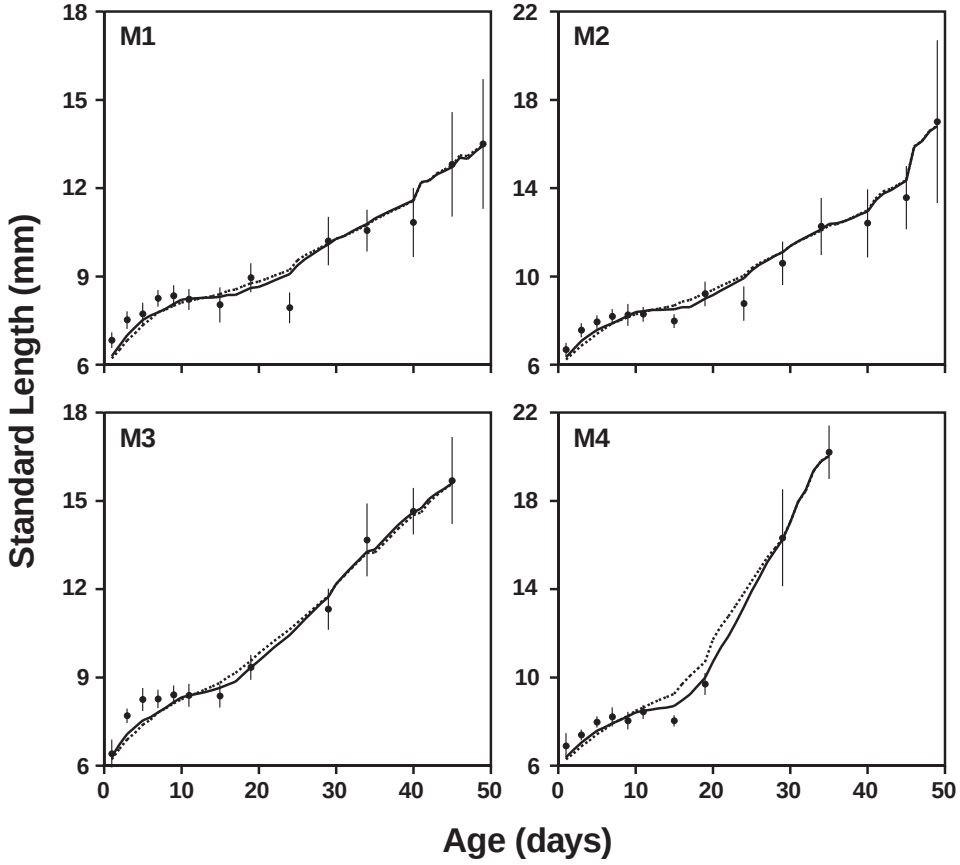

as confirmed by analysis of otolith microstructure of larvae sampled on day 1.

Mean somatic and otolith growth trajectories

Mean somatic growth trajectories within microcosms based on length at capture were described best by fourth-order (M4) and fifth-order (M1, M2, and M3) natural log-transformed equations (Fig.2). These population growth trajectories showed variations in growth rates over time. Among microcosms, fluctuations were similar; fast growth during the yolk-sac stage (0–7 days) was followed by a slow initiation of a curvilinear exponential-type growth period after yolk absorption (Fig. 2). Mean otolith growth trajectories within microcosms based on radius at capture were described best by third-order (M1 and M2) and fourth-order (M3 and M4) natural log-transformed equations (Fig. 3).

Body size – otolith size relationships and the growth effect

Power curves were fitted to the relationships between standard length and otolith radius (Fig. 4). ANCOVA indicated a significant difference among regression slopes ($F_{3,448} = 24.33$, $p < 0.0001$). Multiple comparisons showed a significant difference between all microcosms except between M1 and M2 ($p > 0.05$ for slope and elevation) and between M2 and M3 ($p > 0.05$ for slope and elevation). Differences in slopes of these relationships suggested the presence of a growth effect. According to eq. 1, the magnitude of the growth effect was estimated to be 1.398 (Fig. 5).

Comparison of the TVG method with the BI method at the population level

Mean somatic growth trajectories in the microcosms, as calculated with the TVG method, were higher during the yolk-sac stage and lower between ages 13 and 29 than those calculated with the BI method (Fig. 6). Mean back-calculated length-at-age estimated with the BI method varied from –10.5 to +16.3% of the mean observed length-at-age in microcosms (Fig. 6). Mean back-calculated length-at-age estimated with the TVG method varied from –8.7 to +14.5% of the mean observed length-at-age in microcosms (Fig. 6). These observations suggested that the TVG method described more realistically the observed mean somatic growth trajectories in microcosms. However, there is no significant difference between the slope describing the relationship between mean back-calculated length estimates and mean observed lengths and the theoretical slope of 1 for both methods (Fig. 7).

Comparison of the TVG method with the BI method at the individual level

The number of individual length estimates included within the 95% confidence curves of the fitted growth model was higher when using the TVG method than when using

Table 2. Number of back-calculated length estimates (or increments) included within the 95% confidence curves for individual estimates of the fitted growth curve (Fig. 2) in each microcosm.

	No. of larvae used for back-calculation	Total no. of back-calculated length estimates	No. of length estimates within the 95% confidence curves using the BI method	No. of length estimates within the 95% confidence curves using the TVG method	*p*
M1	129	2452	2325	2339	ns
M2	128	2524	2306	2338	ns
M3	116	2011	1779	1822	0.0268
M4	83	1079	875	946	<0.0001

the BI method in all microcosms (Table 2). This difference is significantly different in M3 (χ^2 = 4.91, df = 1, p = 0.0268) and M4 (χ^2 = 17.72, df = 1, $p < 0.0001$). Moreover, individual growth trajectories from older larvae calculated with the TVG method fitted more accurately the observed mean somatic growth trajectories than those calculated with the BI method in all microcosms (Fig. 8). The maximum difference between the two methods for a single length estimate on a specific day was 39%, based on one larva aged 17 days in M4.

Discussion

Validation of daily otolith increment deposition rate

This study validated the daily nature of otolith increment deposition rate in rainbow smelt larvae. In addition, our observations showed that daily increment formation started at hatching in this species and under these conditions. Examination of otoliths from known-age larvae is one of the most rigorous and reliable methods for validating daily increment deposition (Geffen 1992). Our results differed from the observations of a closely related species, the European smelt (*Osmerus eperlanus*) (Sepúlveda 1994). Using the marginal increment technique on wild-caught larvae, Sepúlveda (1994) assumed that the first discontinuous zone corresponds to the first feeding check.

Comparison of the TVG method with the BI method

This study suggested that the TVG method provided accurate length estimates at previous ages at both the population and individual levels. The TVG method weighted the contribution of each increment in the length calculation using a growth effect factor ($R(W_t - W)$, eq. 3). A small growth increment contributed less to the length increase of larvae than its relative importance in total otolith growth. On the other hand, a large growth increment contributed more to the length increase of larvae in comparison with its relative importance in total otolith growth. The degree of correction is a function of the variation of increment widths and (or) of the magnitude of the growth effect. In the absence of variable increment widths and (or) growth effect, the TGV method corresponds exactly to the BI method.

The proposed model is analogous to proportional-type back-calculation methods as opposed to regression-type methods (see review by Francis 1990). The latter do not allow individual deviation from the mean growth history and do not take into account observed length at capture. In proportional methods, especially when using a BI, the starting and end points of the growth trajectory are reliable. This is important for individual estimations. The use of otolith analysis and the individual-based approach in fishery ecology allows one to perform longitudinal studies and may provide important insights into the recruitment processes. For instance, the analysis of otoliths of survivors can identify the life history stage critical to the determination of the year-class strength. Identification of the stage that is most important for year-class determination allows us to focus on the particular mechanism important to recruitment success (Sissenwine 1984). This study illustrated that the TVG method provided accurate individual length estimates and should be useful for the individual-based approach.

The TVG method demonstrated two desirable characteristics. First, it accounted for variations in growth rates over time by including the growth effect in the back-calculation formula. Campana (1990, eq. 7) presented a regression-type equation to correct TVG; however, when applied to our data

Fig. 7. Relationship between mean back-calculated length and mean observed length using the BI and TVG methods. The four microcosms are pooled. Regression equations, R^2 values, and sample size (N) are reported on each graph.

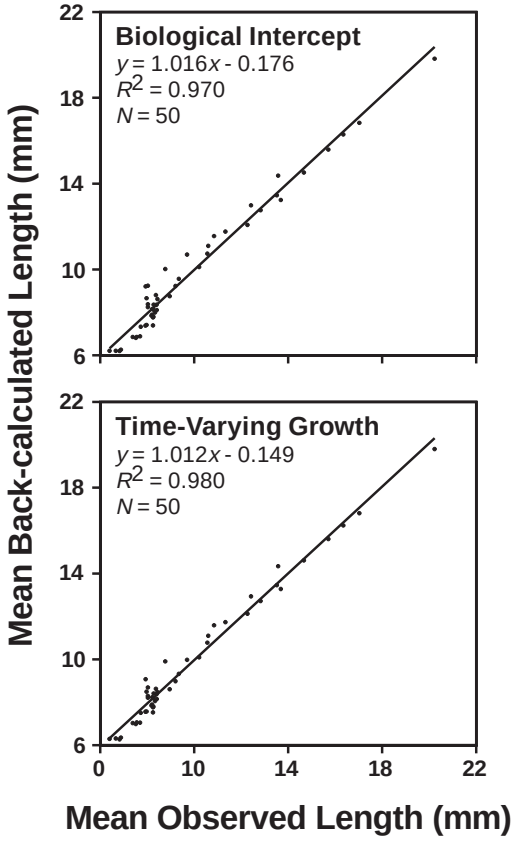

Fig. 8. Observed mean somatic growth trajectories with SDs and back-calculated individual growth trajectories for older larvae in M1, M2, M3, and M4 according to the BI method and TVG methods. Within one microcosm, similar symbols in the middle and the right panels correspond to the same individual. All panels are scaled similarly.

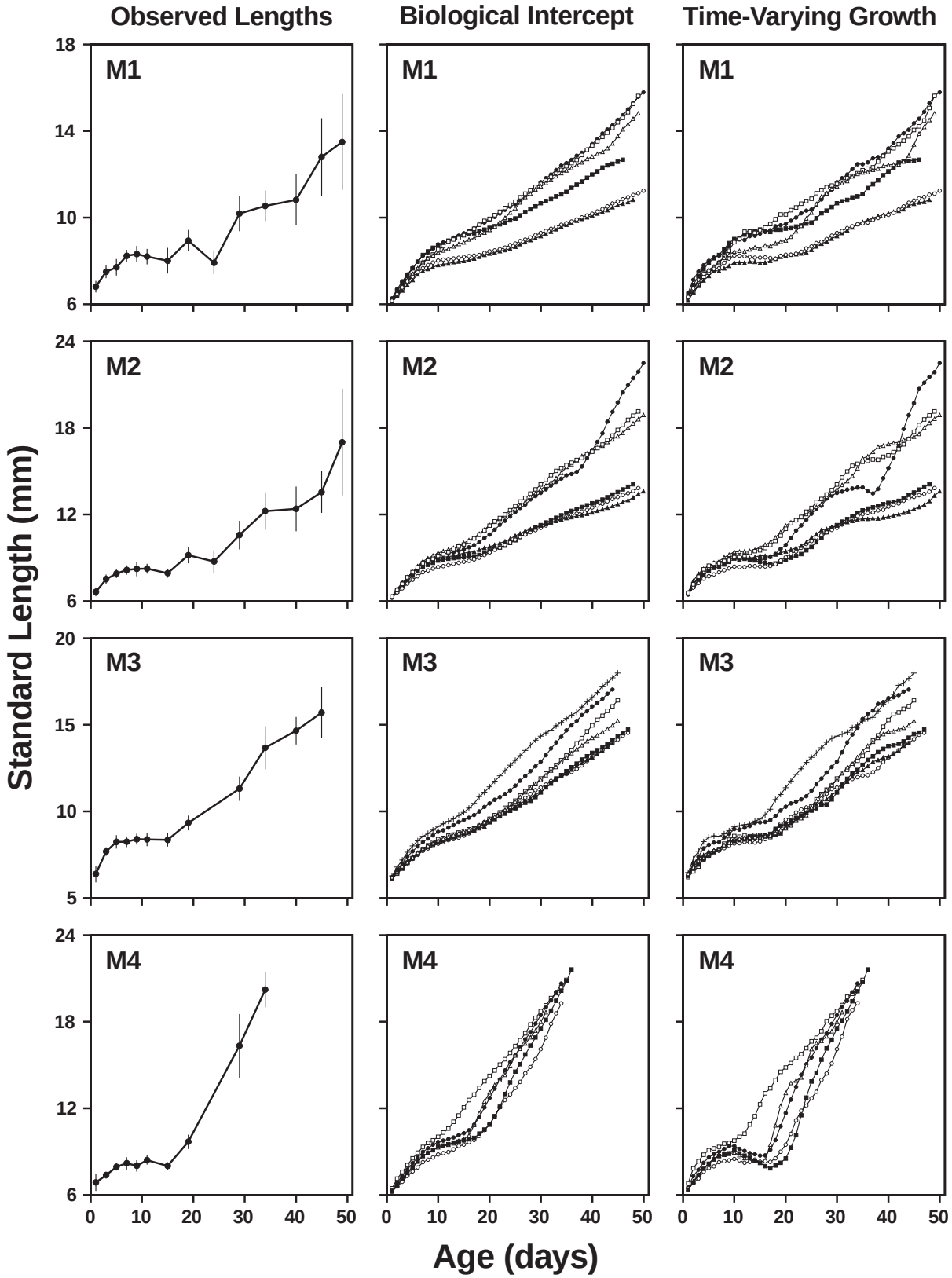

using averaged parameters (L_0 = 5.81 mm, k = 0.65 mmμm^{-1}, R = 1.4, W for days 1–7 = 1.18 μm, W for days 8+ = 1.27 μm), this equation performed poorly. Deviation of the mean somatic growth trajectories from lengths observed in the microcosms varied from 0 to 693%. Second, the TVG method allows one to mathematically determine periods of negative growth. Otolith deposition rate is a conservative process (Mugiya 1987; Mugiya and Oka 1991). In the absence of somatic growth or during periods of negative somatic growth, calcium deposition continues at a reduced rate (Mugiya 1990). Although this feature is particularly useful to obtain true age estimates, it creates errors in length back-calculation when using proportional methods. However, the TVG method is able to accurately estimate negative growth. The quadratic response model proposed by Secor and Dean (1992) accurately predicted mean somatic growth trajectories of larvae reared in the laboratory including inflexion points and negative growth. However, that model was a regression-type method and performed poorly when applied to an independent sample of pond-reared larvae.

The use of the TVG method requires a continuous series of increment widths from the BI to the point of back-calculation, which can be time-consuming to those who wish to back-calculate only a small portion of the early life history (e.g., estimation of recent growth). Another characteristic of the proposed method is the manner in which the growth effect is incorporated into the back-calculation procedure. Secor and Dean (1992) suggested that the growth effect is not expected to be constant across life stages. Hare and Cowen (1995) recommended incorporating such life stage effects in the back-calculation procedures. However, the growth effect is the best single variable available to summarize growth variations across all developmental stages and should not be recalculated for every life history stage. Instead of using a stage-specific growth effect, the method developed here incorporates life stage effects in the back-calculation method by using a stage-specific mean increment width.

In this study, the TVG method provided significantly better estimates for back-calculated length-at-age than the BI method at the individual level. In addition, the TVG method tended to provide more accurate estimates of previous length-at-age than the BI method at the population level, but the difference was not significant. We conclude that the importance of using the TVG method instead of the BI method to back-calculate individual and population body growth trajectories increases with the magnitude of the growth effect and the variation in growth rates over time.

Acknowledgements

This project was supported by grants from the NSERC to J.J.D. We thank Hélène Lemieux, Normand Bertrand, Elizabeth Long, Denis Thivierge, and Serge Higgins for their valuable help in this experiment. We especially thank Guy Trencia (MEF) for providing rainbow smelt eggs. John M. Casselman and an anonymous referee provided helpful reviews on an earlier version of the manuscript. P.S. was funded by NSERC, FCAR (Quebec), and GIROQ fellowships.

References

Bradford, M.J., and Geen, G.H. 1992. Growth estimates from otolith increment widths of juvenile chinook salmon (*Oncorhynchus tshawytscha*) reared in changing environments. J. Fish Biol. **41**: 825–832.

Campana, S.E. 1990. How reliable are growth back-calculations based on otoliths? Can. J. Fish. Aquat. Sci. **47**: 2219–2227.

Campana, S.E., and Jones, C.M. 1992. Analysis of otolith microstructure data. *In* Otolith microstructure examination and analysis. *Edited by* D.K. Stevenson and S.E. Campana. Can. Spec. Publ. Fish. Aquat. Sci. No. 117. pp. 73–100.

Campana, S.E., and Neilson, J.D. 1985. Microstructure of fish otoliths. Can. J. Fish. Aquat. Sci. **42**: 1014–1032.

Casselman, J.M. 1987. Determination of age and growth. *In* The biology of fish growth. *Edited by* A.H. Weatherley and H.S. Gill. Academic Press, New York. pp. 209–242.

Cooper, J.E. 1978. Identification of eggs, larvae, and juveniles of the rainbow smelt, *Osmerus mordax*, with comparisons to larval alewife, *Alosa pseudoharengus*, and gizzard shad, *Dorosoma cepedianum*. Trans. Am. Fish. Soc. **107**: 56–62.

Dodson, J.J., Dauvin, J.-C., Ingram, R.G., and D'Anglejan, B. 1989. Abundance of larval rainbow smelt (*Osmerus mordax*) in relation to the maximum turbidity zone and associated macroplanktonic fauna of the middle St. Lawrence Estuary. Estuaries, **12**: 66–81.

Francis, R.I.C.C. 1990. Back-calculation of fish length: a critical review. J. Fish Biol. **36**: 883–902.

Francis, M.P., Williams, M.W., Pryce, A.C., Pollard, S., and Scott, S.G. 1993. Uncoupling of otolith and somatic growth in *Pagrus auratus* (Sparidae). Fish. Bull. U.S. **91**: 159–164.

Geffen, A.J. 1992. Validation of otolith increment deposition rate. *In* Otolith microstructure examination and analysis. *Edited by* D.K. Stevenson and S.E. Campana. Can. Spec. Publ. Fish. Aquat. Sci. No. 117. pp. 101–113.

Hare, J.A., and Cowen, R.K. 1995. Effect of age, growth rate, and ontogeny on the otolith size – fish size relationship in bluefish, *Potamus saltatrix*, and the implications for back-calculation of size in fish early life history stages. Can. J. Fish. Aquat. Sci. **52**: 1909–1922.

Houde, E.D. 1987. Fish early life history dynamics and recruitment variability. Am. Fish. Soc. Symp. **2**: 17–29.

Laprise, R., and Dodson, J.J. 1989*a*. Ontogeny and importance of tidal vertical migrations in the retention of larval smelt *Osmerus mordax* in a well-mixed estuary. Mar. Ecol. Prog. Ser. **55**: 101–111.

Laprise, R., and Dodson, J.J. 1989*b*. Ontogenic changes in the longitudinal distribution of two species of larval fish in a turbid well-mixed estuary. J. Fish Biol. **35**(Suppl. A): 39–47.

Lea, E. 1910. On the methods used in the herring-investigations. Publ. Circons. Cons. Perm. Int. Explor. Mer. No. 53.

Marshall, S.L., and Parker, S.S. 1982. Pattern identification in the microstructure of sockeye salmon (*Oncorhynchus nerka*) otoliths. Can. J. Fish. Aquat. Sci. **39**: 542–547.

Molony, B.W., and Choat, J.H. 1990. Otolith increment widths and somatic growth rate: the presence of a time-lag. J. Fish Biol. **37**: 541–551.

Mosegaard, H., Svedäng, H., and Taberman, K. 1988. Uncoupling of somatic and otolith growth rates in Arctic char (*Salvelinus alpinus*) as an effect of differences in temperature response. Can. J. Fish. Aquat. Sci. **45**: 1514–1524.

Mugiya, Y. 1987. Phase difference between calcification and organic matrix formation in the diurnal growth of otoliths in the rainbow trout, *Salmo gairdneri*. Fish. Bull. U.S. **85**: 395–401.

Mugiya, Y. 1990. Long-term effects of hypophysectomy on the growth and calcification of otoliths and scales in the goldfish, *Carassius auratus*. Zool. Sci. (Tokyo), **7**: 273–279.

Mugiya, Y., and Oka, H. 1991. Biochemical relationship between otolith and somatic growth in the rainbow trout *Oncorhynchus mykiss*: consequence of starvation, resumed feeding, and diel variations. Fish. Bull. U.S. **89**: 239–245.

Neter, J., Wasserman, W., and Kutner, M.H. 1985. Applied linear statistical models: regression, analysis of variance, and experimental designs. 2nd ed. R.D. Irwin, Homewood, Ill.

Reznick, D., Lindbeck, E., and Bryga, H. 1989. Slower growth results in larger otoliths: an experimental test with guppies (*Poecilia reticulata*). Can. J. Fish. Aquat. Sci. **46**: 108–112.

Rice, J.A., Crowder, L.B., and Binkowski, F.P. 1985. Evaluating otolith analysis for bloater *Coregonus hoyi*: do otoliths ring true? Trans. Am. Fish. Soc. **114**: 532–539.

Schirripa, M.J., and Goodyear, C.P. 1997. Simulation of alternative assumptions of fish otolith–somatic growth with a bioenergetic model. Ecol. Model. **102**: 209–223.

Secor, D.H., and Dean, J.M. 1989. Somatic growth effects on the otolith – fish size relationship in young pond-reared striped bass, *Morone saxatilis*. Can. J. Fish. Aquat. Sci. **46**: 113–121.

Secor, D.H., and Dean, J.M. 1992. Comparison of otolith-based back-calculation methods to determine individual growth histories of larval striped bass, *Morone saxatilis*. Can. J. Fish. Aquat. Sci. **49**: 1439–1454.

Secor, D.H., Dean, J.M., and Baldevarona, R.B. 1989. Comparison of otolith growth and somatic growth in larval and juvenile fishes based on otolith length/fish length relationships. Rapp. P.-v. Réun. Cons. Int. Explor. Mer, **191**: 431–438.

Sepúlveda, A. 1994. Daily growth increments in the otoliths of European smelt *Osmerus eperlanus* larvae. Mar. Ecol. Prog. Ser. **108**: 33–42.

Sissenwine, M.P. 1984. Why do fish populations vary? *In* Exploitation of marine communities. *Edited by* R.M. May. Springer-Verlag, New York. pp. 59–94.

Volk, E.C., Wissmar, R.C., Simentad, C.A., and Eggers, D.M. 1984. Relationship between otolith microstructure and the growth of juvenile chum salmon (*Oncorhynchus keta*) under different prey rations. Can. J. Fish. Aquat. Sci. **41**: 126–133.

Wright, P.J., Metcalfe, N.B., and Thorpe, J.E. 1990. Otolith and somatic growth rates in Atlantic salmon parr, *Salmo salar* L: evidence against coupling. J. Fish Biol. **36**: 241–249.

Xiao, Y. 1996. How does somatic growth rate affect otolith size in fishes? Can. J. Fish. Aquat. Sci. **53**: 1675–1682.

Zar, J.H. 1987. Biostatistical analysis. 2nd ed. Prentice-Hall, Englewood Cliffs, N.J.